Supporting Information for

Switching of magnetic properties by topotactic reaction in a 1D CN-bridged Ni(II)-Nb(IV) system

Michał Heczko and Beata Nowicka*

Faculty of Chemistry, Jagiellonian University, Gronostajowa 2, 30-387 Kraków, Poland
*beata.nowicka@uj.edu.pl

Contents:

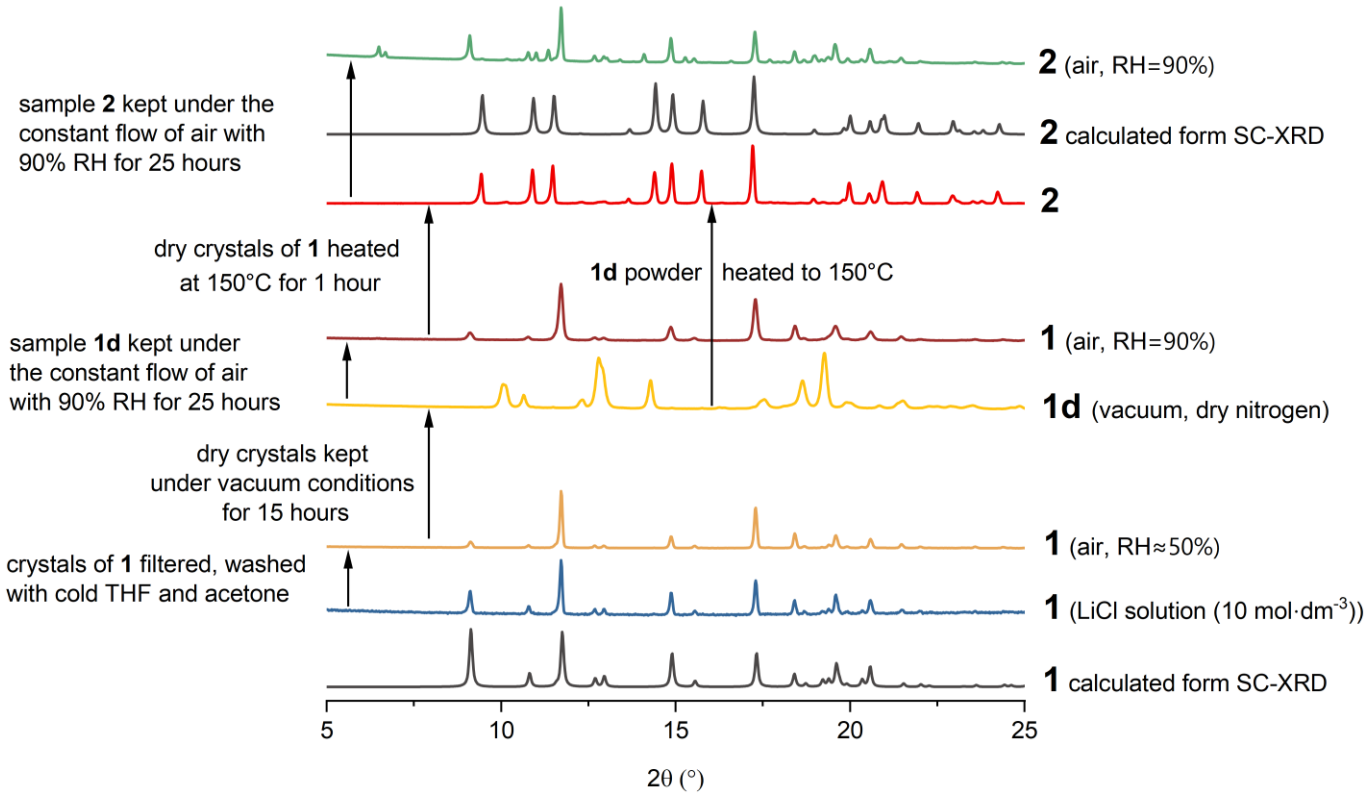

Figure S1. Powder X-ray diffraction patterns of compound **1** measured under various conditions in comparison with the patterns of **1** and **2** calculated from SC-XRD models at 100 K. Top graph (green) shows that the transition from **2** to **1** is accompanied by partial recrystallization to the neutral Ni_2Nb polymer (ref. 32).

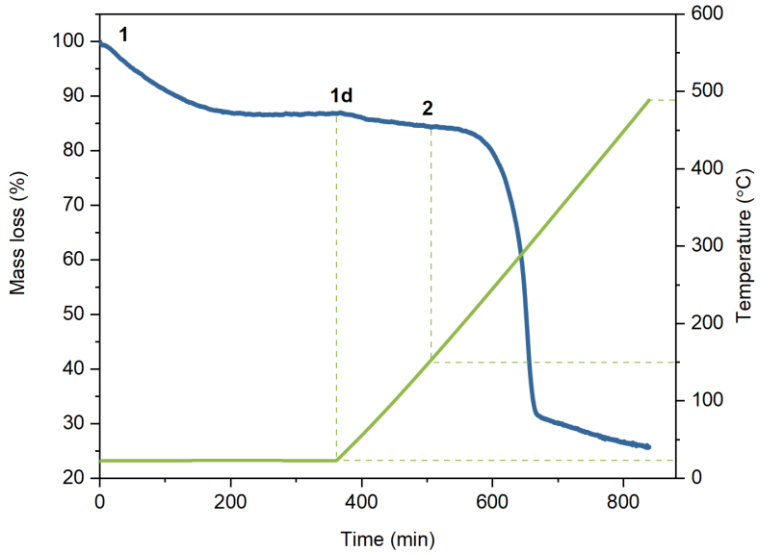

Figure S2. Thermogravimetric analysis for compound **1** measured under dry nitrogen flow (20 cm^3/min). The measurement began from the 6-hour isothermal step, then the temperature was increased from 25°C to 490°C at the heating rate of 2°C/min.

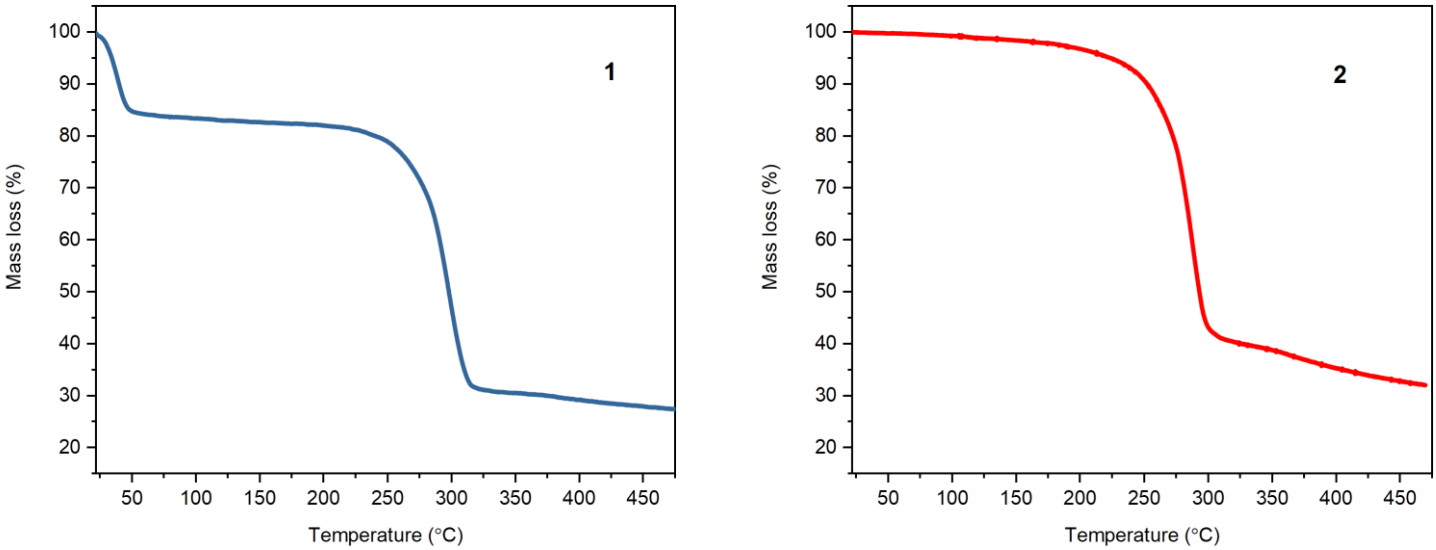

Figure S3. Thermogravimetric analysis for compounds **1** and **2** measured under dry nitrogen flow (20 cm^3/min) at the heating rate of 2°C/min.

Table S1. Continuous Shape Measure (CShM) parameters (the lowest four) for the octa-coordinated niobium centers in compounds **1** and **2**.

		SAPR-8	TDD-8	BTPR-8	JSD-8
1	Nb1	0.114	2.430	2.088	4.952
2	Nb1	1.807	0.374	1.975	2.761

CShM = 0 indicates an ideal geometry; SAPR-8 = square antiprism, TDD-8 = triangular dodecahedron, BTPR-8 = biaugmented trigonal prism, JSD-8 = snub disphenoid.

Table S2. Continuous Shape Measure (CShM) parameters (the lowest four) for the hexa-coordinated nickel centers in compounds **1** and **2**.

		HP-6 (D_{6h})	PPY-6 (C_{5v})	OC-6 (O_h)	TPR-6 (D_{3h})
1	Ni1	30.182	28.837	0.154	16.236
2	Ni1	29.992	28.786	0.193	15.950

CShM = 0 indicates an ideal geometry; HP-6 = hexagon; PPY-6 = pentagonal pyramid; OC-6 = octahedron; TPR-6 = trigonal prism.

Table S3. Continuous Shape Measure (CShM) parameters for the tetra-coordinated lithium centers in compounds **1** and **2**.

		SP-4 (D_{4h})	T-4 (T_d)	SS-4 (C_{2v})	vTBPY-4 (C3v)
1	Li1	27.363	0.611	6.707	3.094
2	Li1	31.775	1.841	7.020	3.654

CShM = 0 indicates an ideal geometry; SP-4 = square, T-4 = tetrahedron, SS-4 = seesaw, vTBPY-4 = vacant trigonal bipyramid.

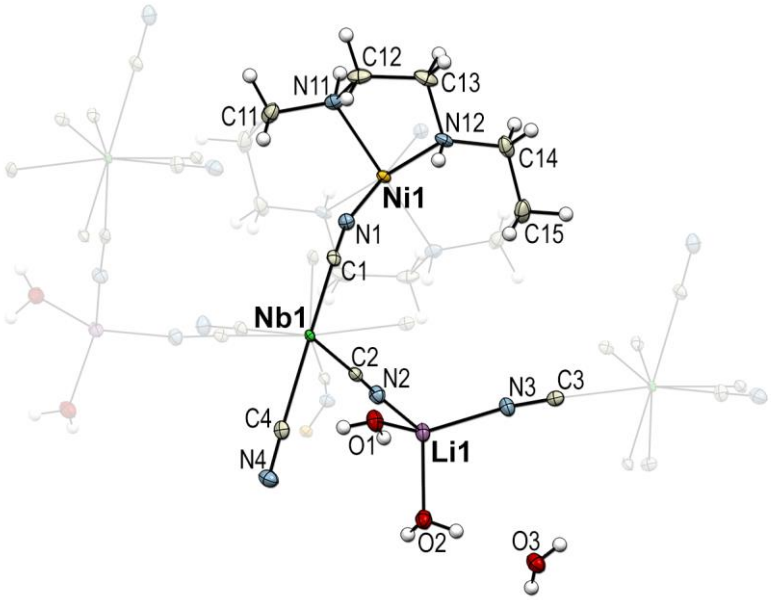

Figure S4. The asymmetric unit of 1; thermal ellipsoids shown at 50% probability.

Table S4. Selected interatomic distances and bond angles in the structures of 1 and 2.

	1	2
Distance between metal centers (Å)	Ni1-Nb1: 5.4169(3)	Ni1-Nb1: 5.3276(2)
Ni-N_{CN} distance (Å)	Ni1-N1: 2.1044(17)	Ni1-N1: 2.0643(16)
Ni-N_{cyclam} distance (Å)	Ni1-N11: 2.0823(17) Ni1-N12: 2.0718(17)	Ni1-N11: 2.0843(18) Ni1-N12: 2.0683(18)
Ni-N≡C angle (°)	Ni1-N1≡C1: 162.33(16)	Ni1-N1≡C1: 156.28(16)
Nb-C≡N angle (°)	Nb1-C1≡N1: 174.55(17)	Nb1-C1≡N1: 177.94(17)

Table S5. Hydrogen-bonds geometry in compound **1**.

D—H···A	D—H (Å)	H···A (Å)	D···A (Å)	D—H···A (°)
C11—H11B···N1	0.99	2.69	3.219(3)	114
N12—H12···O3^{iii}	1.00	2.11	3.032(2)	152
O1—H1B···N4^{v}	0.79(3)	2.17(3)	2.941(2)	169(3)
O2—H2A···N2^{v}	0.78(3)	2.46(3)	3.158(2)	149(2)
O2—H2B···O3	0.79(3)	1.96(3)	2.743(2)	176(3)
O3—H3A···N3^{vi}	0.74(3)	2.45(3)	3.177(2)	167(3)
O3—H3B···N4^{vii}	0.79(3)	2.08(3)	2.832(3)	159(3)

Symmetry codes: (iii) −*x*+1, −*y*+1, −*z*+1; (v) −*x*+1, −*y*+2, −*z*+1; (vi) −*x*+3/2, *y*, −*z*+3/2; (vii) *x*+1/2, −*y*+2, *z*+1/2.

Table S6. Hydrogen-bonds geometry in compound **2**.

D—H···A	D—H (Å)	H···A (Å)	D···A (Å)	D—H···A (°)
N12—H12···N4^{i}	1.00	2.50	3.354(3)	144
O1—H1A···N4^{ix}	0.78(3)	2.00(3)	2.778(2)	175(2)

Symmetry codes: (i) -*x*+1, *y*, −*z*+3/2; (ix) −*x*+1/2, −*y*+3/2, −*z*+2.

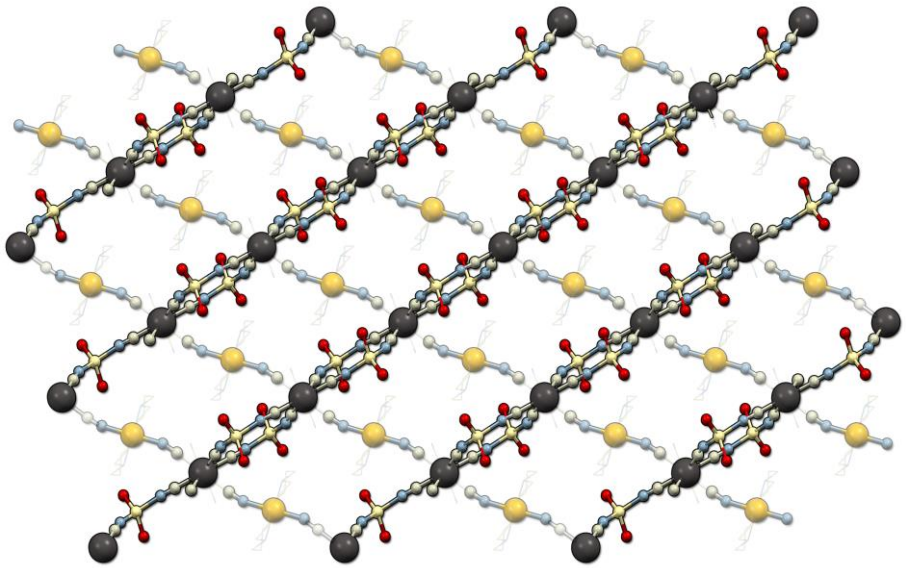

Figure S5. The structure of **1** viewed along [010] crystallographic direction showing the chains composed of $[Nb(CN)_8]^{4-}$ and $[Li(H_2O)_2]^{+}$ ions connected through the $[Ni(cyclam)]^{2+}$ complex ion.

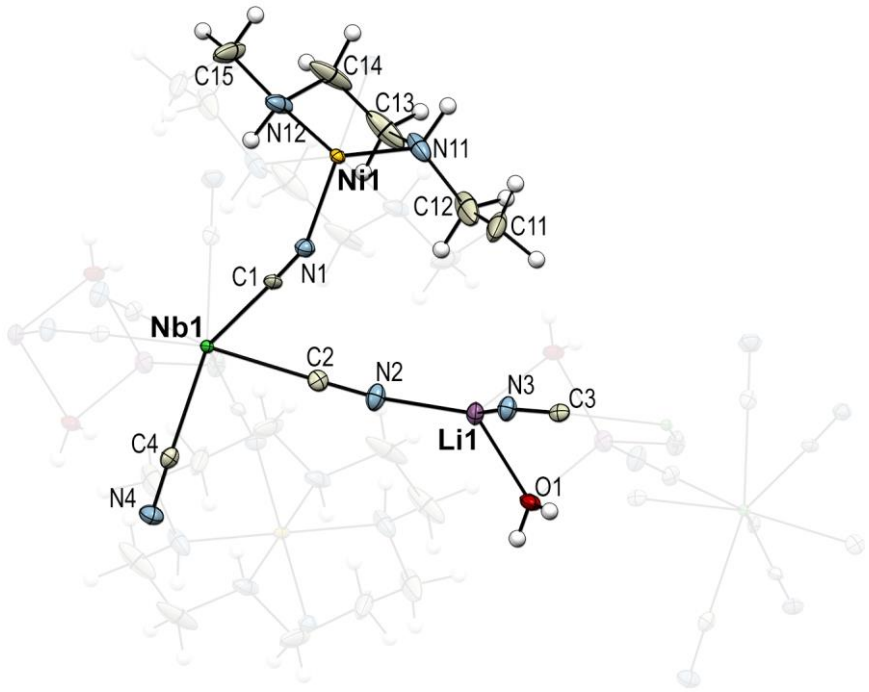

Figure S6. The asymmetric unit of 2; thermal ellipsoids shown at 50% probability.

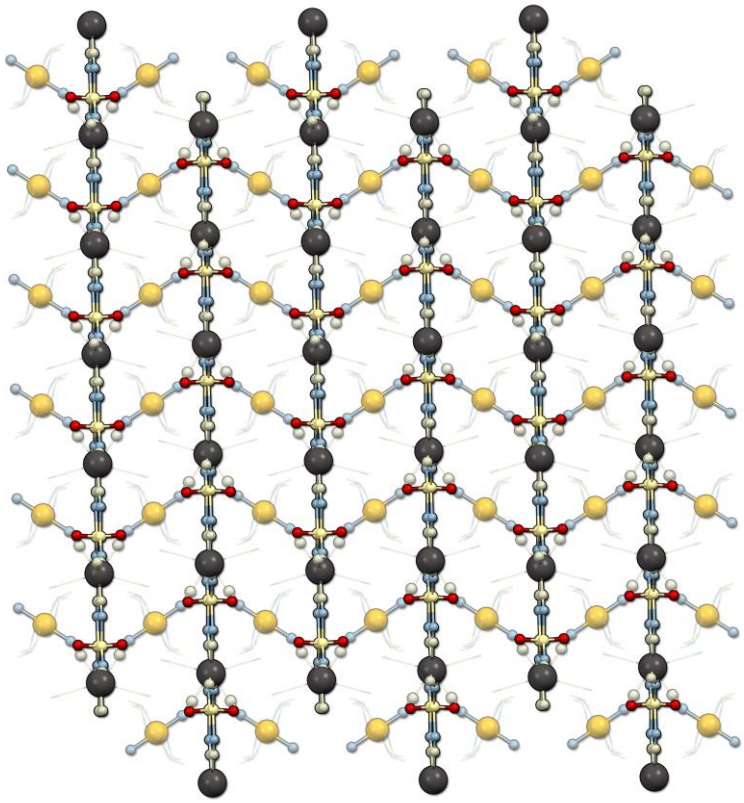

Figure S7. The structure of 2 viewed along [100] crystallographic direction showing the parallel layers composed of $[Nb(CN)_8]^{4-}$ and $[Li_2(H_2O)_2]^{2+}$ ions connected through the $[Ni(cyclam)]^{2+}$ complex ion.

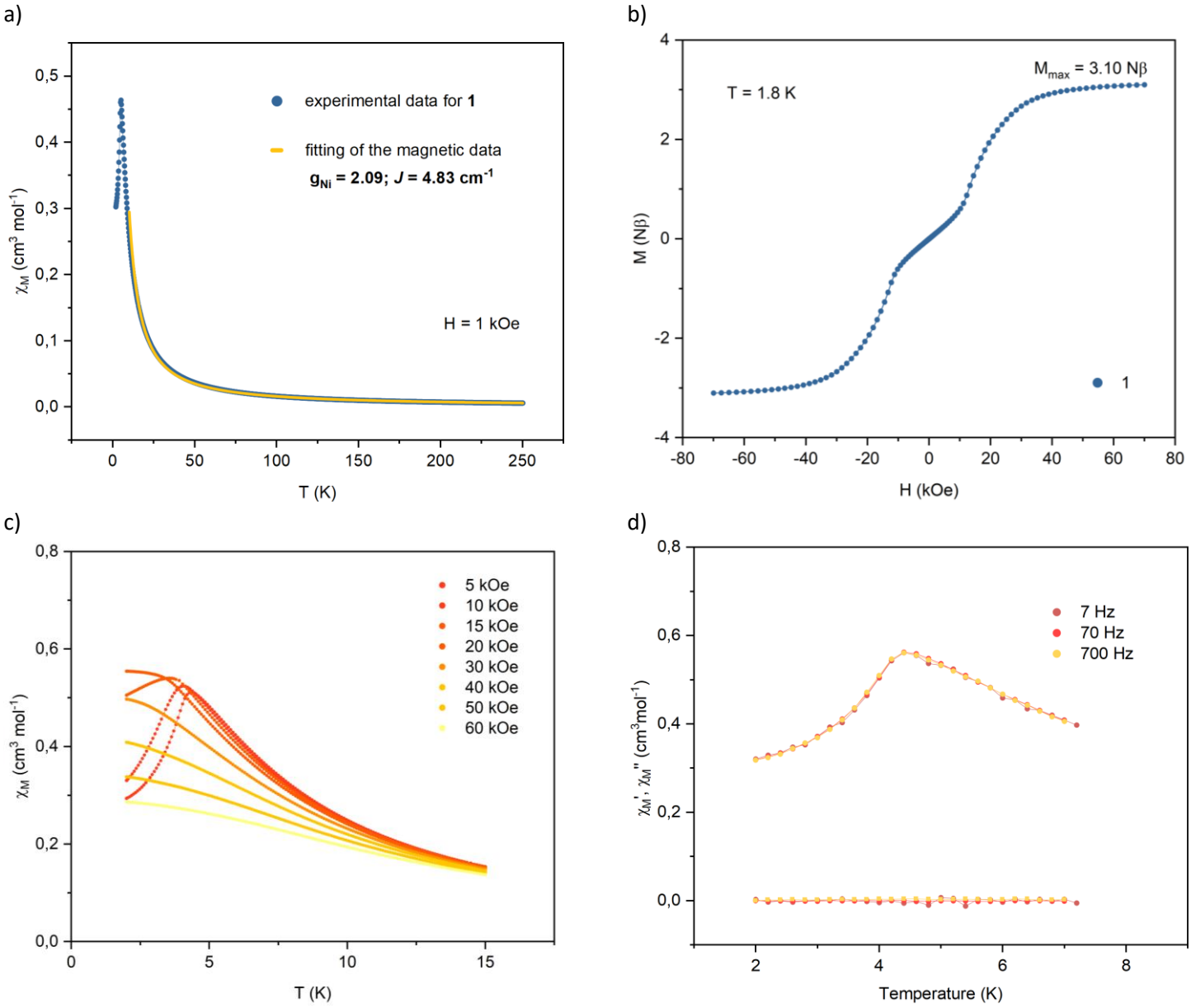

Figure S8. Magnetic properties of **1**: (a) DC susceptibility at 1 kOe, line represents fitting above 10K with fixed g_{Nb} = 2.00; (b) magnetization at 1.8K, (c) field-cooled (FC) magnetic susceptibility at different fields, (d) AC susceptibility (H_{AC} = 1 Oe, H_{DC} = 0).

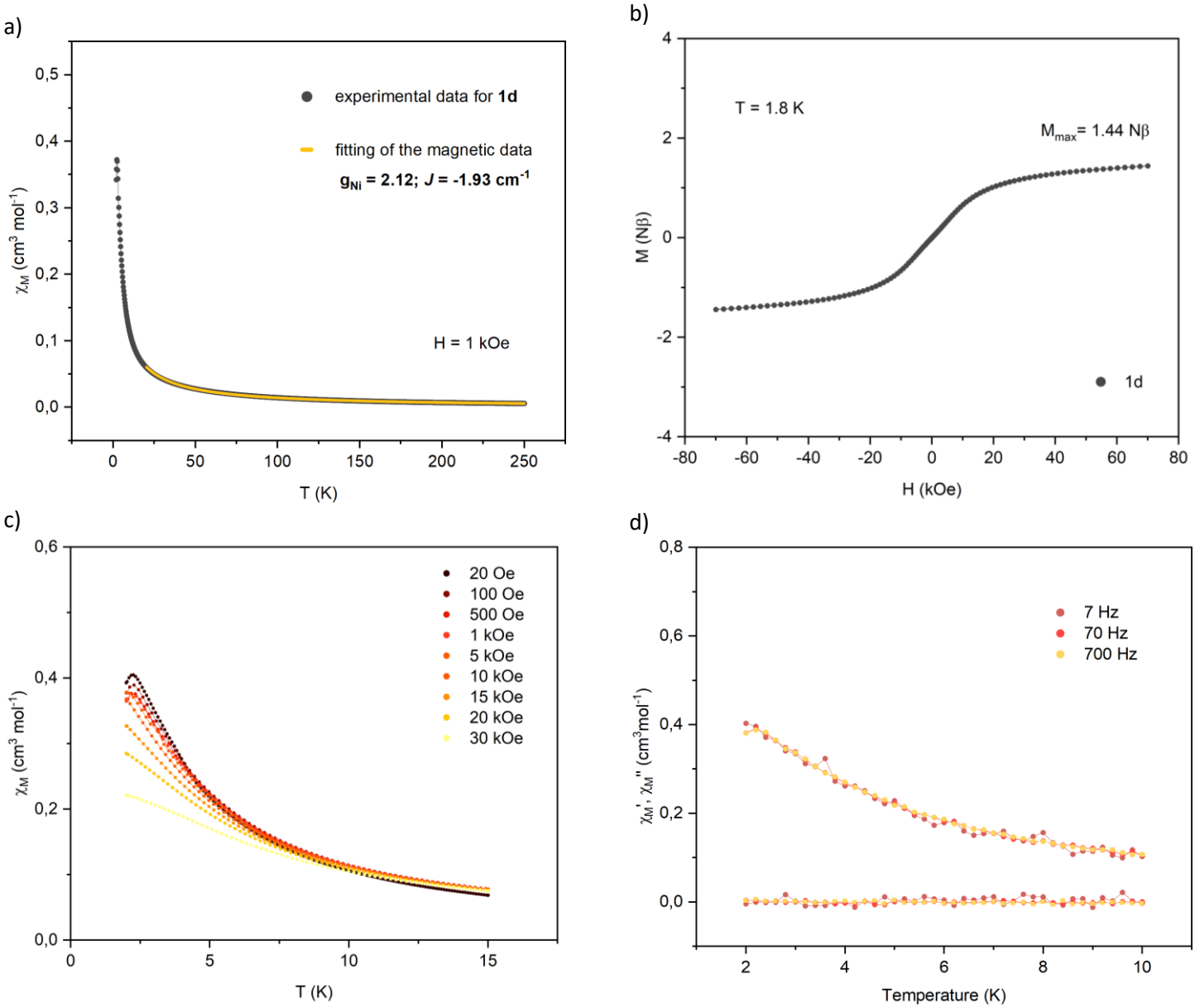

Figure S9. Magnetic properties of **1d**: (a) DC susceptibility at 1 kOe, line represents fitting above 30K with fixed g_{Nb} = 2.00; (b) magnetization at 1.8K, (c) field-cooled (FC) magnetic susceptibility at different fields, (d) AC susceptibility (H_{AC} = 1 Oe, H_{DC} = 0).

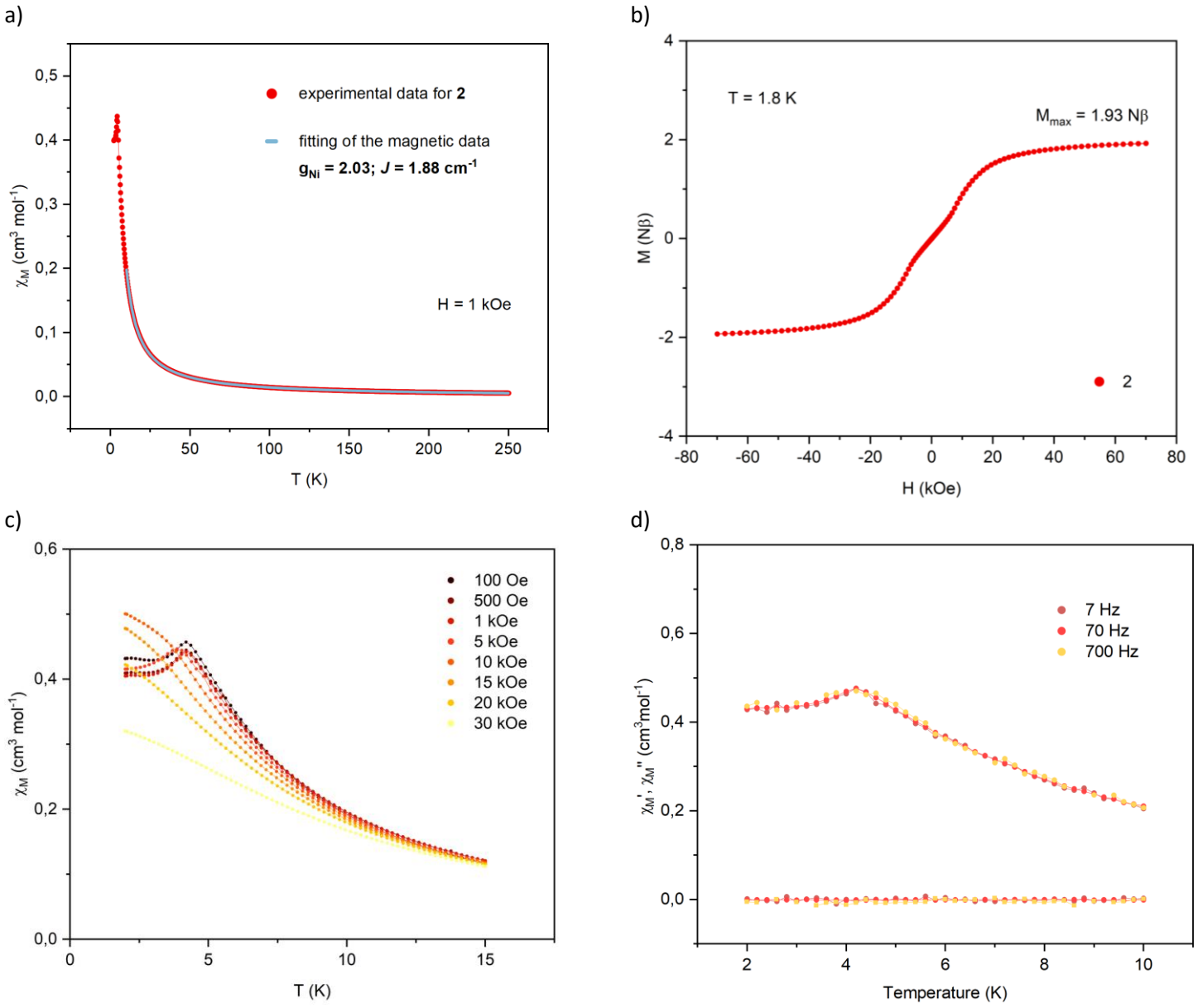

Figure S10. Magnetic properties of **2**: (a) DC susceptibility at 1 kOe, line represents fitting above 10K with fixed g_{Nb} = 2.00; (b) magnetization at 1.8K, (c) field-cooled (FC) magnetic susceptibility at different fields, (d) AC susceptibility (H_{AC} = 1 Oe, H_{DC} = 0).

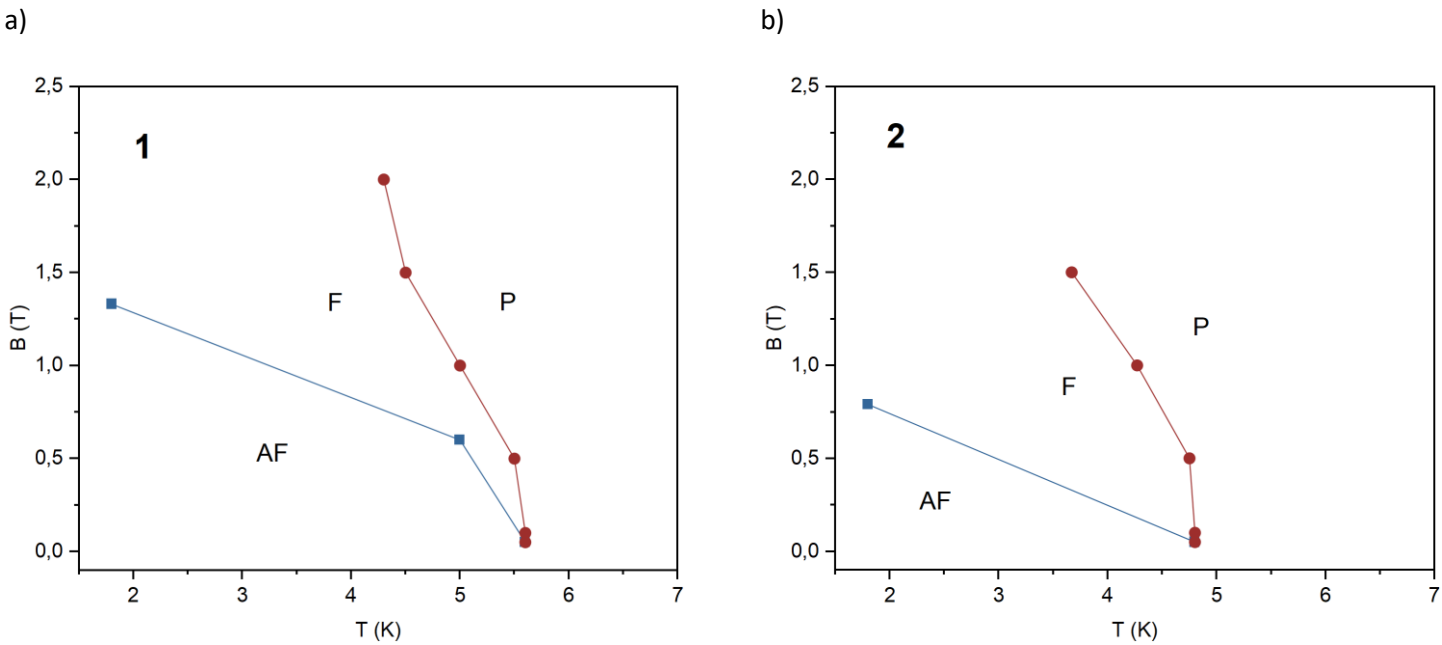

Figure S11. Magnetic phase diagrams for compounds **1** and **2**; AF - antiferromagnetic phase, F - ferromagnetic phase, P - paramagnetic phase. Squares mark the critical field of metamagnetic transition derived from magnetization *vs.* field measurements at indicated temperatures, circles mark the critical temperature derived from magnetic susceptibility *vs.* temperature measurements at different magnetic fields. The connecting lines are drawn to guide the eye.

Table S7. Comparison of magnetic exchange constants and bridge angles in Ni^{II}-Nb^{IV} CN-bridged systems.

Compound	dimensionality	J (cm^{-1})	Ni-N≡C angle (°)	reference
$[Ni(4\text{-bromopyridine})_4]_2[Nb(CN)_8]\cdot 2H_2O$	(3D)	9.6	176.3	36
$[Ni(pyrazole)_4]_2[Nb(CN)_8]_3\cdot 4H_2O$	(3D)	8.1	164.4	7
$Li_2[Ni(cyclam)][Nb(CN)_8]\cdot 7.5H_2O$ (**1**)	(1D)	4.8	162.3	this work
$Li_2[Ni(cyclam)][Nb(CN)_8]\cdot 2H_2O$ (**2**)	(1D)	1.9	156.3	this work